The histone H3K9 methylation and RNAi pathways regulate normal nucleolar and repeated DNA organization by inhibiting formation of extrachromosomal DNAs

Jamy C. Peng and Gary H. Karpen*

Department of Genome Biology, Lawrence Berkeley National Lab, One Cyclotron Road, Berkeley, CA 94720

Department of Molecular and Cell Biology, University of California at Berkeley, Berkeley, CA 94720

* Correspondence: karpen@fruitfly.org

Abstract

In order to identify regulators of nuclear organization, Drosophila mutants in the *Su(var)3-9* histone H3K9 methyltransferase, RNAi pathway components, and other regulators of heterochromatin-mediated gene silencing were examined for altered nucleoli and positioning of repeated DNAs. Animals lacking components of the H3K9 methylation and RNAi pathways contained disorganized nucleoli, ribosomal DNA (rDNA) and satellite DNAs. The levels of H3K9 dimethylation (H3K9me2) in chromatin associated with repeated DNAs decreased dramatically in *Su(var)3-9* and *dcr-2* (*dicer-2*) mutant tissues compared to wild type. We also observed a substantial increase in extrachromosomal repeated DNAs in mutant tissues. The disorganized nucleolus phenotype depends on the presence of Ligase 4 (*Lig4*), and ecc DNA formation is not induced by removal of cohesin. We conclude that H3K9 methylation of rDNA and satellites, maintained by Su(var)3-9, HP1, and the RNAi pathway, is necessary for the structural stability of repeated DNAs, which is mediated through suppression of non-homologous end joining (NHEJ). These results suggest a mechanism for how local chromatin structure can regulate genome stability, and the organization of chromosomal elements and nuclear organelles.

Introduction

Nuclei and chromosomes maintain specific and dynamic architectures, which are required for a variety of essential functions[1]. Nuclear bodies are involved in diverse biological processes and exhibit dynamic mobility, and individual chromosomes are organized into distinct domains within interphase nuclei[2]. However, little is known about how their formation and activities are regulated. The organization of DNA in eukaryotic nuclei goes far beyond packaging into nucleosomes and chromosomes. Chromosomes in the metazoan interphase nucleus are comprised of two types of cytologically and functionally distinct chromatin, euchromatin and heterochromatin[3], which have been correlated with patterns of post-translational histone modifications. For example, heterochromatin is rich in histone H3K9 methylation and lacks many histone acetylations, whereas euchromatic histones are highly acetylated and methylated at H3K4[4]. Strong correlations exist between these histone modifications and functions such as gene regulation, chromosome inheritance, and replication timing[5].

The first indication that chromosome organization can affect gene expression stems from the discovery of position effect variegation (PEV) in *Drosophila* by H.J. Muller[6]. PEV describes the epigenetic inactivation or silencing of a euchromatic gene that has been positioned close to or within heterochromatin, or a heterochromatic gene moved to distal chromosome locations. PEV is exquisitely sensitive to the dosage of genetic modifiers, known as suppressors and enhancers of variegation (*Su(var)*s and *E(var)*s)[7]. PEV modifiers regulate heterochromatin formation and functions. For example, the *Su(var)3-9* family encodes a histone methyltransferase (HMTase) responsible for H3K9 methylation, and *Su(var)2-5* encodes heterochromatin protein1 (HP1). Methylated H3 K9 and Su(var)3-9 bind to HP1, providing a molecular mechanism for maintaining the silenced epigenetic state[4]. Components of the RNA interference (RNAi) pathway also act as *Su(var)s* that influence silencing of tandem repeats[8]. Recent studies have shown that RNAi pathway and dsRNA are required for the initial recruitment of H3K9 methyltransferases, and establishment and maintenance of heterochromatin[9].

The nucleolus, the site of ribosome assembly, is an example of an essential nuclear organelle. The nucleolus organizer region (NOR ribosomal DNA) is embedded in the heterochromatin in most eukaryotes. *Drosophila melanogaster* contains 160-240 tandemly repeated rDNA genes in the X and Y heterochromatin. Single rDNA genes inserted into euchromatin are able to form mini-nucleoli, suggesting that nucleolus formation may be determined by a self-assembly process that is initiated by rRNA transcription[10]. Epigenetic regulation of rDNA transcription is well documented in yeast, plant, and mammalian systems. For example, a mammalian nucleolar remodeling complex (NoRC) regulates heterochromatin formation and rRNA expression by controlling histone H4 deacetylation, H3K9 dimethylation, and

de novo DNA methylation at rDNA[11]. Also, nucleolar dominance occurs when only one NOR forms a nucleolus in interspecies hybrids[12]. Increases in rDNA copy number (magnification) occur in yeast and flies with low rDNA content; this process is likely mediated by unequal sister chromatid recombination[13]. Finally, mutations in a protein that regulates silencing in *S. cerevisiae* (SIR2, also affecting rDNA magnification) results in extrachromosomal (ecc) rDNA formation, which is thought to affect cell senescence and aging[14].

It is surprising that rDNA produces the overwhelming majority of RNAs in the cell, despite its association with 'silenced' heterochromatin. This paradox suggests that the evolutionarily conserved positioning of NORs in heterochromatin may regulate important, unknown features of nucleolus formation. Here, we test the hypothesis that heterochromatin and associated proteins regulate nucleolus formation in *Drosophila*. Our results demonstrate that a subset of *Su(var)* proteins, including the *Su(var)*3-9 HMTase, HP1, and the RNAi pathway, are required for the normal organization of nucleoli and satellite DNAs in the nucleus, and suppress ecc DNA formation from repeated DNAs through the non-homologous end-joining pathway (NHEJ), and perhaps other repair mechanisms.

Results

Multiple nucleoli are present in *Su(var)* mutant cells

We used indirect immunofluorescence (IF) to examine nucleolar organization in whole-mount (three dimensional) imaginal disc tissues and polytene larval salivary glands from wild type and *Su(var)* mutant larvae (see Materials and Methods). Staining with an antibody to fibrillarin, a component of the rRNA processing machinery[15], confirmed that wild type polytene and diploid cells contain single nucleoli (Figure 1). In contrast, salivary gland cells from animals homozygous for mutations in the Su(var)3-9 histone H3K9 methyltransferase or HP1/*Su(var)* 2-5 genes contained between 1 and 12 nucleoli (Figure 1a, Table 1). The average numbers of nucleoli in mutant cells (*Su(var)3-9*^{null} = 2.7, *Su(var)3-9*^{1699} = 5.0, *HP1*^{null} = 2.8) were significantly higher than in wild type (avg=1, Supplemental Table 1). Increases in nucleolar numbers were accompanied by a proportional increase in both nuclear and nucleolar volumes, even though the ratios remained constant (data not shown). Irregularly-shaped, multi-lobed nucleoli were also observed in 44% of *Su(var)3-9*^{null} mutant diploid imaginal disc cells, versus only 10% in wild type cells (Figure 1b).

Fibrillarin staining in salivary glands of *Su(TDA-PEV)1650* (Figure 1a) and *Su(var)2-10/dPIAS* (data not shown) mutant cells displayed the multiple nucleoli phenotype, whereas nucleoli in six other *Su(var)* mutants and two Polycomb-Group (PcG) mutants were unaffected (Supplemental Table 1). We conclude that many but not all regulators of gene silencing are required for the formation of a normal, single nucleolus.

Ectopic nucleoli in *Su(var)* mutants contain rDNA

Multiple, ectopic nucleoli associated with *Su(var)* mutations could result from dispersion or fission of nucleolar material, initially formed around a single rDNA cluster, or ectopic nucleoli could be nucleated independently by mislocalized rDNA. These hypotheses were distinguished by performing simultaneous IF for fibrillarin and FISH for rDNA on whole-mount tissues. Wild type polytene nuclei predominantly displayed single sites of rDNA within the fibrillarin signal (Figure 2a). Polytene nuclei from homozygous *Su(var)3-9*, *HP1*, and *Su*(*TDA-PEV)1650* mutants contained multiple, dispersed rDNA foci associated with ectopic nucleoli (Figure 2a). Multiple rDNA foci were also present in diploid disc cells from *Su(var)3-9*^{null} mutants, unlike the single focus observed in wild type disc cells (Figure 2b). Quantitative analysis showed that 33% of the *Su(var)3-9*^{null} mutant diploid cells contained more than one rDNA site (average=1.44±0.72), compared to only 2% of wild type cells (average=1±0.1, Figure 2c). These results demonstrate that ectopic nucleoli in *Su(var)* mutants are nucleated independently by mislocalized rDNA. The presence of multiple rDNA foci in disc cells indicates that the lobed nucleoli in mutant diploid

nuclei (see above) correspond to multiple nucleoli, which are difficult to resolve by fibrillarin staining and light microscopy (nuclei are 1/10 the size of polytene nuclei).

Su(var)3-9 mutants disrupt the organization of other repeated DNAs

The severe disruption to rDNA and nucleolar organization raised the possibility that the 3-dimensional spatial relationships of other heterochromatic DNAs are also affected by *Su(var)* mutations. To address this question, FISH analysis on whole mount salivary glands was performed using probes to tandemly-repeated satellite DNAs (Figure 3a), which localize to the heterochromatic chromocenter in polytene nuclei.[16] An average of two sites were observed in wild type polytene nuclei for satellites 1.688 and 1.686, compared to 3 sites in *Su(var)3-9*^{null} mutant cells (Figure 3b, c; $p<0.001$). Similar observations were made with satellites AACAC and AATAT (data not shown). Distances between signals for each satellite increased significantly in *Su(var)3-9*^{null} mutants (1.688 = 9-fold, 1.686 = 3-fold; Figure 3b, d; $p<0.001$). We conclude that heterochromatic repeated DNAs become dispersed and disorganized in *Su(var)3-9* mutants, as observed for rDNA and nucleoli. In addition, the satellite DNA and rDNA signals are distributed throughout the nucleus and are not colocalized, suggesting that the mislocalized DNAs were not restricted to a specific nuclear compartment.

H3K9me2 levels at rDNA and satellite DNAs decrease significantly in *Su(var)3-9* mutants

Heterochromatic nucleosomes in a variety of organisms, including *Drosophila*, are enriched for the H3K9me2 modification. Thus, HP1 and Su(var)3-9 could control rDNA and nucleolar organization indirectly by regulating the flanking heterochromatin, or they could act directly on the rDNA chromatin. To address this question, we determined if rDNA and satellite DNAs contained methylated H3K9, and if this modification was disrupted in *Su(var)3-9* mutants. Combined IF and FISH studies indicated that H3K9me2 partially overlapped with rDNA in wild type disc cells, and was significantly reduced in *Su(var)3-9*^{null} mutants (Figure 4a).

We performed chromatin immunoprecipitation (ChIP) to analyze H3K9 methylation levels in rDNA chromatin and heterochromatin at higher resolution. Quantitation showed that rDNA, 5S rDNA, and both satellite DNAs are associated with H3K9me2 in wild type disc cells, and that this modification was not well represented at actin and HDAC3 (single copy gene controls; Figure 4b). The levels of H3K9me2 differed among regions of the rDNA, but in all cases the enrichment was significant. Most importantly, the level of H3K9me2 on all repeated DNAs decreased substantially in chromatin isolated from *Su(var)3-9*^{null} mutant discs. The reductions in H3K9me2 levels varied among the different repeats and within the rDNA (6- to 226-fold, Figure 4b, top), most likely reflecting known redundancy in the HMTases responsible for this modification in flies[17]. In sum, the ChIP and combined IF-FISH results suggest that the effects of Su(var)3-9 on rDNA and nucleolar organization are mediated through the chromatin structure of the rDNA itself, rather than solely through the flanking heterochromatin.

H3K4me2 and H3K9ac have been characterized as modifications associated with active or open chromatin. ChIP analysis showed that chromatin associated with repeated DNAs contained low levels of H3K9ac (Figure 4c) and H3K4me2 (Figure 4d), which in general were not significantly reduced in *Su(var)3-9*^{null} mutants, most notably in the rDNA. Exceptions were significant increases in 5S rDNA H3K9ac levels in the mutants ($p=0.024$), and H3K4me2 decreases for the 1.688 satellite ($p=.037$).

Su(var)3-9 mutations cause significant increases in the amount of extrachromosomal repeated DNA

How do chromatin changes alter the organization of repeated DNAs and nucleoli? Loss of H3K9me2 could generate extrachromosomal (ecc) DNA through intra-chromatid recombination, or chromatin decondensation could cause dispersal of repeated DNAs in the nucleoplasm. To test these hypotheses we looked for the presence of ecc DNA in mutant and wild type cells. PCR was used to evaluate the levels of ecc DNA in ‘Hirt’ supernatants, a method developed to isolate viral

episomes and other non-genomic, extrachromosomal DNAs[18]. Wild type polytene tissues contain ecc 5S rDNA and satellite DNA 1.688, as observed previously[19], but had very low levels of ecc 18S/5.8S/28S rDNA (Figure 5a). The amount of ecc DNA increased dramatically in *Su(var)3-9*^{null} mutant tissues versus wild type for all tested regions of the rDNA (46- to 78-fold), and the 1.688 satellite (20-fold) (Figure 5b; wild type versus mutant, $p<0.05$ for all regions), which was not observed for the single copy genes actin and HDAC. For diploid cells, quantitative analysis showed that ecc repeated DNAs were ~2-fold higher in *Su(var)3-9* mutant tissues than in wild type (Figure 5c; $p < 0.05$ for all regions). The lower enrichments for ecc DNA observed in mutant diploid cells in comparison to polytene cells likely results from the absence of endoreplication and loss of ecc DNA during mitosis (see Discussion). We conclude that loss of H3K9me2 from chromatin containing repeated DNAs results in ecc DNA formation, and that the increased ecc rDNA leads to the assembly of ectopic nucleoli.

Mutants in the RNAi pathway contain disorganized nucleoli, loss of H3K9me2 from rDNA, and increase in extrachromosomal rDNA

The targeting of H3K9me2 by the RNAi pathway[9], and the presence of small RNAs homologous to the 1.688 satellite and other repeats[20], led us to examine whether RNAi mutants also contain disorganized nucleoli. All RNAi loci examined displayed significantly increased nucleolus numbers when mutated, in comparison to wild type ($p<0.001$ for all except for *hls*$^{\Delta 215}$, $p<0.08$; Supplementary Table 1 and Figure 6a and b). To determine if the RNAi pathway regulates nucleolus and rDNA organization through H3K9 methylation, we focused on the Dicer-2 gene (*dcr-2*), which has been shown to affect production of siRNAs more than miRNAs[21]. ChIP analysis of *dcr-2*^{L811fsx} mutants revealed significant H3K9me2 reduction in the rDNA; unlike *Su(var)3-9* mutants, reductions were not observed for 5S rDNA and satellite 1.688 ($p<0.05$, Figure 6c). IF analysis showed that the H3K9me2 is concentrated in the heterochromatin in wild type diploid nuclei, but is more broadly distributed in *dcr-2*^{L811fsx} homozygous mutants (Figure 6d). Finally, ecc rDNA increased significantly in *dcr-2*^{L811fsx} mutants (13 to 29-fold, Figure 6e), consistent with ectopic nucleolus formation and increases observed in response to loss of H3K9me2 in *Su(var)3-9* mutants (Figure 5).

***Lig4* mutations partially suppress the disorganized nucleolus phenotype observed in *Su(var)*3-9 mutant**

Formation of ecc DNA from repeated DNA most likely arises from somatic recombination. Support for this model comes from the demonstration that *sir2*-dependent ecc rDNA formation in *S. cerevisiae* requires the RAD52 complex[14,22]. Efforts to identify recombination proteins required for ecc DNA formation in *Drosophila* have been unsuccessful[23], and *Drosophila RAD52* homologs have not been identified by genomic analysis. A recent study in mammals identified Ligase IV, an essential regulator of non-homologous end joining (NHEJ), as necessary for ecc DNA formation[24]. Therefore, we used fibrillarin IF to examine nucleolar organization in polytene nuclei from *Lig4* mutants (transheterozygous for null alleles 57 and 29), as well as *Lig4*; *Su(var)3-9*^{null} double mutants. Removal of *Lig4* does not increase the number of nucleoli compared to wild type, but does suppress the formation of multiple nucleoli when combined with *Su(var)3-9* mutants (Figure 7). The average nucleolus number in double mutant nuclei is 1.7± 0.8 (N = 83), which is significantly lower than the number in *Su(var)3-9*^{null} mutant nuclei (2.7, $p<0.001$). This result demonstrates a role for Lig4 and the NHEJ pathway, and perhaps other repair machinery, in ecc DNA formation from repeated DNAs in Drosophila.

The level of repeat-associated cohesins is reduced in *Su(var)3-9*^{null} mutants, but a cohesin mutation does not increase extrachromosomal DNA formation

Ecc rDNA formation in *S. cerevisiae* coincides with cohesin displacement from the rDNA spacer region by directional rDNA transcription, suggesting that normal sister chromatid cohesion inhibits ecc DNA formation[25]. H3K9me2 and the HP1 homolog SWI6 are required for cohesin

recruitment in *S. pombe*[26]. Thus, potential recruitment of cohesin to pericentric heterochromatin by the H3K9me pathway in *Drosophila* could also regulate structural integrity of repeated DNA and prevent ecc DNA formation. ChIP analysis showed that levels of the SMC1 cohesin subunit[27] were significantly reduced in *Su(var)3-9*^{null} chromatin (16 to 29 % of wild type level, Figure 8a). However, the amount of ecc DNA isolated from the single available cohesin mutant, *smc1*^{exc461}, did not differ significantly from wild type (Figure 8b). These results demonstrate that Su(var)3-9 and the H3K9 methylation pathway are required for cohesin recruitment at repeated DNAs. However, cohesin is not essential for repression of ecc DNA formation in *Drosophila*, unlike its requirement in *S .cerevisiae*.

Discussion

The H3K9 methylation and RNAi pathways regulate the organization of repeated DNAs and the nucleolus

Patterns of post-translational histone modifications have been correlated with regulation of gene expression[5]. However, recent studies have demonstrated that associations between modification patterns and genome functions are not simple. The 'silent' H3K9 methylation mark is also linked with transcriptional elongation in coding regions[28], and human and *Drosophila* centromeric chromatin contains modification patterns that are distinct from 'canonical' euchromatin and heterochromatin[29]. Our knowledge of the impact of chromatin structures on other aspects of nuclear functions, such as the 3-dimensional organization of sequences, chromosomes, and nuclear organelles, is also limited.

Here we show that the Su(var)3-9 H3K9 methyltransferase, its binding partner HP1, and the RNAi pathway are required for the normal organization of rDNA, satellite DNAs, and the nucleolus in *Drosophila*. When animals lack these components, repeated DNAs and nucleoli become dispersed to multiple nuclear locations. ChIP and IF-FISH demonstrated that wild type rDNA and satellites are highly enriched for the H3K9me2 modification, consistent with previous studies of rDNA and other repeats in *S. pombe*[30,31]. In addition, we show that H3K9me2 levels in chromatin associated with repeated DNAs are strongly reduced in *Su(var)3-9* and *dcr-2* mutant animals. Finally, we observed significantly increased amounts of extrachromosomal repeated DNAs in these mutants. We conclude that the H3K9 methylation and RNAi pathways directly regulate nuclear architecture, by affecting chromatin structure and repressing ecc DNA formation of rDNA and satellites.

We showed that other proteins involved in heterochromatin structure and function are also required to maintain the structural integrity of repeated DNA and nucleoli. dPIAS is an E3 ligase of the SUMOylation pathway[32,33], suggesting that regulation of other heterochromatin pathways besides H3K9 methylation may be required to maintain a single nucleolus. This argument is supported by a recent observation of nucleolar disruption in mouse blastocysts after Ubc9 (SUMO E2-conjugating enzyme) depletion[34]. Further analysis is required to determine whether dPIAS and other *Su(var)s* (e.g. *Su(TDA-PEV)1650*) function through the H3K9 methylation pathway.

It is important to note that numerous tested *Su(var)*s, including two alleles of *SUV4-20*, had no effect on nucleolar organization. This observation suggests that H3K9me2, not H4K20me3 (methylated by SUV4-20, whose activity requires H3K9me2), is the primary histone modification responsible for maintaining repeated DNA integrity. Finally, it is interesting that *dsir2* mutants do not display the ectopic nucleolus phenotype, since the SIR2 NAD-dependent histone deacetylase is required for repressing ecc rDNA formation in *S. cerevisiae*[14]. We conclude that rDNA organization and nucleolar architecture are regulated by only a subset of proteins involved in heterochromatin structure and function.

Differential effects of components of the H3K9 methylation and RNAi pathways

We observed significantly-increased amounts of ecc satellite 1.688 in *Su(var)3-9* mutants (Figure 5), but not in *dcr-2*^{L811fsx} mutants (Figure 6e). Differential requirements for repeat structure

regulation was also suggested by the behavior of 5S rDNA, a tandem array located in euchromatin; *Su(var)3-9* mutants displayed a 17-fold H3K9me2 reduction at the 5S rDNA locus, but only a 2-fold increase in ecc DNA increase, and *dcr-2* mutants had a 3.2-fold reduction in H3K9me2 and no increased ecc DNA. We conclude that Dicer-2 regulates H3K9me2 levels and ecc DNA formation at some but not all repeated DNAs, in contrast to the broad impact of Su(var)3-9. The *dcr-2*^{L811fsx} mutation was shown to be the strongest allele in terms of its effect on siRNA production[21]. Thus, Dicer-2 and other RNAi components may preferentially direct H3K9 methylation of rDNA via the siRNA pathway in *Drosophila*, whereas other repeats are regulated by different pathways or components.

The mislocalization of H3K9me2 in *dcr-2* mutant diploid cells (Figure 6d) is particularly striking and surprising, since H3K9me2 is not detectable in RNAi mutants in *S. pombe*[30] and levels are severely reduced in Drosophila polytene tissues[8]. We conclude that in the absence of Dicer-2, overall levels of H3K9me2 are not reduced, and instead the specificity of siRNA-mediated targeting of this modification to heterochromatin is altered.

Impact of Su(var)3-9 and H3 K9 methylation on cells and animals

Mice deleted for both Su(var)3-9 genes exhibit genome instability and early embryonic lethality[35]. Despite very low levels of H3K9me2 in *Su(var)3-9*^{null} flies, these animals are viable and fertile, presumably due to the presence of a redundant H3 Lys9-methyltransferase[17]. Our studies show that the absence of *Su(var)3-9* has dramatic effects on cells, in terms of nuclear and nucleolar organization, and the integrity of repeated DNAs. The presence of fibrillarin around ectopic rDNA and the increased nucleolar volume suggest that transcription and processing of ribosomal RNA occurs in ectopic nucleoli. Similarly, ectopically-integrated rDNA is able to form functional 'mini-nucleoli'[10], and can also rescue defects in X-Y pairing in male meiosis caused by deletion of the endogenous rDNA[36]. These observations suggest that increased nucleolar volumes, ecc rDNA, and rRNA do not cause significant growth abnormalities. However, there are likely to be developmental or physiological phenotypes yet to be discovered. For example, increased ecc rDNA in *Su(var)3-9* mutants may affect cell senescence, as observed for *sir2* mutants in *S. cerevisiae*[14]. We have also observed that non-recombinant chromosomes display significantly increased levels of meiotic non-disjunction in *Su(var)*3-9^{null} females (GHK, unpublished), consistent with previous studies demonstrating that heterochromatin is involved in achiasmate segregation[37,38]. More detailed analysis need to be performed on *Su(var)3-9* mutant animals to determine the impact of significantly reduced H3K9 methylation, and increased ecc DNA and ectopic nucleoli, on the organism.

Another explanation for the absence of dramatic phenotypic abnormalities in *Su(var)3-9*^{null} animals arises from our observation that diploid tissues display lower levels of ectopic nucleoli and ecc DNA in comparison to polytene cells. Ecc DNAs should lack functional centromeres and would be poorly transmitted in rapidly dividing diploid cells, but would be retained in the non-mitotic polytene nuclei. Thus, the absence of obvious phenotypic defects in *Su(var)3-9*^{null} animals may occur because ecc DNA and ectopic nucleoli, and perhaps other cellular abnormalities, are less severe in mitotically dividing cells, which are the source of most adult tissues in *Drosophila*.

A model for the regulation of nuclear architecture by the Su(var)3-9/H3K9 methylation pathway

Our findings demonstrate that chromatin structures regulated by Su(var)3-9, HP1, the RNAi pathway, and H3K9 methylation are required to repress extrachromosomal DNA formation in tandemly repeated, heterochromatic sequences, similar to their roles in repression of gene expression (PEV) (Figure 9). *HP1* mutant cells display increased restriction enzyme accessibility in heterochromatin, consistent with chromatin decondensation and loss of gene silencing[39]. We propose that H3K9 methylation, and perhaps other heterochromatic properties and components, generate a chromatin structure that normally restricts access of DNA repair proteins to repeated DNA substrates, or locally inhibits their activity (Figure 9). The observation that mutations in *Lig4*,

an essential player in the NHEJ pathway, partially suppress ectopic nucleolus formation in *Su(var)3-9*^{null} nuclei supports a role for DNA repair. It is somewhat surprising that the NHEJ pathway, rather than homologous recombination, would participate in ecc DNA formation from repeats. However, it is possible that Ligase 4 acts in other repair pathways in Drosophila, as suggested by Lig4's association with proteins required for double strand break repair and V(D)J site-specific recombination[40]. Alternatively, ecc repeated DNA formation in Drosophila may not involve homologous recombination. Finally, we also showed that cohesins are significantly reduced at repeated DNA chromatin in *Su(var)3-9*^{null} nuclei. However, complete loss of the SMC1 cohesin component did not lead to increases in ecc DNA. This suggests that cohesins do not suppress ecc DNA formation in Drosophila, contrary to observations in *S. cerevisiae*[25].

It is likely that decondensation and increased recombination occur in both diploid and polytene cells in response to loss of H3K9 methylation (Figure 9). Decondensation and aberrant 'looping' of rDNA due to loss of this pathway is likely to be the primary cause of the 'lobed' nucleolar phenotype observed in diploid cells. Decondensation is probably a prerequisite for increasing access of repair proteins to repeated DNAs in mutant polytene cells, but the much larger increases in ecc DNAs and ectopic nucleoli probably reflect a stronger requirement for repression of DNA recombination or NHEJ in endoreplicating tissues. In highly endoreplicated nuclei, euchromatic sequences are present in thousands of copies, satellite sequences are replicated at most twice, and rDNA is replicated to intermediate levels (~250 copies)[16]. This differential endoreplication results in stalled forks at euchromatin-heterochromatin junctions[41], and presumably between the rDNA and adjacent sequences. Stalled forks and associated single-stranded DNA in *S. cerevisiae* have been shown to provide substrates for recombination among repeated DNA to form ecc DNA[42], and could play similar roles in polytene cells that lack *Su(var)3-9* and H3K9 methylation. Diploid cells would not be expected to generate as much ecc DNA and ectopic nucleoli as endoreplicating cells, because DNA copy numbers are much lower, and they would not contain as many stalled replication forks. Furthermore, ecc DNA levels in diploid nuclei would not be retained, since they are likely to be lost during cell division; retention of ecc DNAs in polytene nuclei would be higher, since they are non-mitotic.

Other examples of heterochromatic silencing mechanisms affecting recombination have been reported. Combinations of heterozygous *Su(var)* mutations in *Drosophila* result in elevated levels of meiotic recombination in heterochromatin[43], and loss of gene silencing components in budding and fission yeasts increases both meiotic and somatic recombination in the rDNA[30,44]. Similarly, the G9a H3K9 methyltransferase regulates accessibility of the V(D)J recombination machinery during mouse lymphocyte development[45]. Here, we expand on previous studies by demonstrating the impact of these mechanisms on nucleolar organization and the spatial arrangement of repeated sequences in the nucleus of a developing animal. In addition, these findings may have broader significance to genome stability; the extensive sequence homology inherent to repeated DNAs would presumably generate translocations and other chromosome aberrations in somatic and/or germ cells if exchange was not repressed by heterochromatic structures.

Acknowledgements

The authors thank James Birchler (*hls*$^{\Delta 215}$), Richard Carthew (*DCR2*^{L811fsx}), Dale Dorsett (SMC1 antibody), Scott Hawley (*smc1*^{exc461}), Fenbiao Gao (*Ago2*^{51B}), Thomas Jenuwein (H3K9me2 antibody), Mike Pollard (fibrillarin antibody), Gunter Reuter (*Su(var)3-9* alleles 6 and 17), and Jasper Rine (*dSir2*^{17}) for reagents, Samara Weiss for experimental contributions, Abby Dernburg for help with FISH experiments, and Austin Blanco (formerly Metamorph) for assistance with volumetric analysis. We thank Needhi Bhalla, Abby Dernburg, Sylvia Erhart, Patrick Heun, Barbara Mellone, Aki Minoda, and Weiguo Zhang for helpful discussions and critical comments on the manuscript. This work was supported by NIH grant R01GM061169.

Materials and Methods

Fly stocks

All fly stocks were raised at 22 °C. Information regarding the fly strains are described in Supplementary Table 1. We received the *suv4-20*, *Pc*, *Ph*, *Lig4*, *aub*, *Spn-E*[1], and *piwi* flies from the Bloomington stock center, and the *dcr-2* P element insertion from the Harvard fly center.

Antibodies

The human anti-fibrillarin antibody (dilution 1:500 in IF) was a gift from Mike Pollard, and the rabbit anti-H3K9me2 antibody (dilution 1:100 in IF and 1:1000 in ChIP) was provided by Thomas Jenuwein[46]. Rabbit antibodies against H3 Lys9-acetyl and H3K4me2 were purchased from Upstate. Rabbit antibodies against SMC1 (1:1000 in ChIP) were a gift from Dale Dorsett[47].

IF, FISH, and IF-FISH of whole-mount tissues and squashed tissues.

FISH was performed as described in Dernburg,1996[38] using 100 ng of each probe. In combined IF-FISH experiments, IF was performed before the FISH treatment. FISH probes were made with nick translation and terminal labeling, using materials published in Karpen et al., 1988[38].

Volumetric, distance, and colocalization analysis

All images were captured using an Applied Precision Deltavision Workstation and deconvolved using the conservative algorithm with 8 iterations. SoftWorx software was used to measure colocalization and distances, which were normalized to the nuclear diameter. The deconvolved, stacked images were converted to TIFF files and 3-dimensionally reconstructed, and volumes of nuclei (DAPI signals) and nucleoli (fibrillarin signals) were measured using Metamorph software. All statistical comparisons and p values were calculated using the two-sample t test, assuming two-tailed and unequal variance.

Chromatin Immunoprecipitation (ChIP)

Protocols were modified from Austin et al.[48] Brain and disc tissues were dissected from fifty 3rd instar larvae, then fixed in 1.8% paraformaldehyde/ PBST for 10 minutes at room temperature. The tissues were washed twice in cold PBST, then one time in cold TE and RIPA lysis buffer. Sonication in a 1 ml volume was performed with a Branson Sonifier 450 (6 times with a 90 % duty cycle and a 5.5 power output; each cycle included a 2-minute rest interval) or the Bioruptor (Diagenode; 30 second on-off cycles for 12 minutes at high intensity). 300 µl of the sheared chromatin was used for IP. The input and IP'd DNAs were resuspended in 100µl, 1µl of which was used in 25-µl PCR reactions that were terminated at the logarithmic phase of amplification. Signals from the PCR products were captured using a BioRad Gel Doc workstation and analyzed with the Quantity One software. Values were calculated as a percentage of input. Real-time PCR was also performed to confirm our results. Primer sequences are available upon request.

Variabilities existed between individual H3K9me2 ChIP experiments. While all the experiments showed the same trends of H3K9me2 level reduction in *Su(var)3-9*^{null} chromatin (statistical analysis always showed significant reduction), the values differed. Both the cytology and ChIP results agreed that H3K9me2 levels are significantly lower in *Su(var)3-9*^{null} chromatin.

Hirt extrachromosomal DNA isolation and detection

About 200 larvae were frozen in liquid nitrogen, ground with mortar and pestle, resuspended in 500 µl Hirt lysis buffer (0.6% SDS; 10mM EDTA, pH 8)[18], then incubated at room temperature for 10 to 20 minutes. 125µl of 5M NaCl was added to the extract, which was incubated at 4°C overnight (8 to 20 hours). The larval extract was centrifuged at 14,000g and 4°C for 40 minutes. The supernatant was phenol-chloroform extracted 3 times and the Hirt DNA was ethanol-precipitated. To check for any genomic DNA contamination, the Hirt supernatant before

pheno-chloroform extraction was methanol-acetic acid fixed on slides and examined by DAPI staining [49]. The precipitated Hirt DNA was also examined by standard electrophoresis agarose gel and ethidium bromide staining. 200ng of Hirt DNA was used for each PCR reaction to probe for specific DNAs. Signals from the PCR products were captured and analyzed using a BioRad Gel Doc workstation and the Quantity One software. For diploid tissues, 50 sets of brains and discs were dissected and lysed with 100μl Hirt lysis buffer. The Hirt DNA isolated from diploid cells contains some genomic DNA, so the relative amount of ecc DNAs in mutant and wild type tissues were quantitated by comparing the results from separate PCR reactions for Hirt DNA and genomic DNA preparations.

Figure Legends

Figure 1 *Su(var)* mutants contain multiple nucleoli. a) IF with antibodies against the nucleolus marker fibrillarin (red) in whole-mount nuclei of salivary glands from wild type, *Su(var)3-9*^{null}, *Su(var)3-9*^{1699}, *HP1*^{null} and *Su(TDA-PEV)1650* homozygous mutants. Wild type cells have one nucleolus, whereas the mutants display multiple nucleoli. Blue = DAPI. Scale bars are 10μm. b) Fibrillarin IF in whole-mount imaginal disc and brain tissues from wild type and *Su(var)3-9* mutants are shown. The single, wild type nucleolus (N=51) tended to be round, whereas nucleoli in the mutants are irregular (lobed) and larger. Quantitative analysis showed that 44% of *Su(var)3-9*^{null} mutant nuclei contained lobed nucleoli (N=55), versus 10% for wild type ($p<0.001$). The scale bars are 5μm.

Figure 2 *Su(var)* mutants have dispersed rDNA foci, each of which forms an ectopic nucleolus. a) Fluorescence in situ hybridization (FISH) for rDNA (red) and IF for fibrillarin (green) were performed on whole-mount salivary glands from wild type, *Su(var)3-9*^{null}, *Su(var)3-9*^{1699}, *HP1*^{null}, and *Su(TDA-PEV)1650* homozygous mutants. Blue = DAPI. There is a single site of rDNA in >98% of wild type nuclei, whereas the *Su(var)* mutant nuclei contain multiple rDNA foci, which are all surrounded by fibrillarin. Scale bars are 15μm. b) Combined rDNA FISH (red) and fibrillarin IF (green) analysis of whole-mount imaginal disc and brain tissues from wild type and *Su(var)3-9*^{null} mutant larvae. Wild type nucleoli contain a single, compact rDNA focus, whereas *Su(var)3-9*^{null} mutants frequently display multiple rDNA foci. Scale bars are 3μm. c) Quantitative analysis of the number of rDNA foci in wild type and *Su(var)3-9*^{null} diploid nuclei. 98% of wild type cells (N=96) contain one rDNA signal, compared to 67% of *Su(var)3-9* null nuclei, and the percent with 2, 3, and 4 rDNA signals was 24%, 7%, and 2%, respectively (average $=1.44 \pm 0.73$ rDNA foci per mutant nucleus, N=53, $p<0.001$).

Figure 3 Satellite DNA organization is disrupted in *Su(var)3-9*^{null} mutant nuclei. a) Locations of rDNA and satellite DNAs in the *Drosophila melanogaster* genome (not to scale). The rDNA is located in the heterochromatin of the X and Y sex chromosomes, the 1.688 satellite (359-bp repeats) are next to the X rDNA, and the 1.686 satellite is in the heterochromatin of chromosomes 2 and 3. b) FISH was performed on whole-mount polytene salivary glands isolated from wild type and *Su(var)3-9*^{null} mutants. In wild type nuclei, specific satellite DNAs are localized at single sites, and the different satellite signals are close to each other. In *Su(var)3-9*^{null} mutant nuclei, individual satellite DNAs are dispersed to multiple sites and are not clustered with other satellites. Gray is DAPI, FISH probe colors correspond to the diagram in a. Scale bars are 15μm. c) The number of 1.688 and 1.686 foci were significantly higher in mutant nuclei compared to wild type ($p<0.001$). d) Distances between satellite signals were quantitated in 3-dimensional reconstructions. The intra-satellite distances in *Su(var)3-9*^{null} mutant nuclei were significantly higher than in wild type ($p<0.001$).

Figure 4 Analysis of histone modifications in chromatin containing repeated DNA in wild type and *Su(var)3-9*^{null} cells. a) IF using antibodies that specifically bind H3K9me2 (red) combined with FISH for rDNA (green) in squashed diploid nuclei. In wild type nuclei, rDNA chromatin partially overlaps with the H3K9me2 signals (correlation coefficient $= 0.61 \pm 0.08$), and the amount of overlap was significantly reduced in *Su(var)3-9*^{null} mutants (correlation coefficient $= 0.40 \pm 0.03$; $p<0.01$). Scale bar is 3μm. b) Chromatin immunoprecipitation (ChIP) analysis of H3K9me2 levels in wild type and *Su(var)3-9*^{null} mutant imaginal disc tissues. The graph shows H3K9me2 levels for the repeated DNAs examined by PCR, standardized to actin and HDAC single copy controls (see Materials and Methods); values were averages of 5 ChIP experiments. In wild type cells, the 1.688 satellite (359-bp repeats), 5S rDNA (in chromosome 2 euchromatin), and the rDNA on the sex chromosomes contain significant enrichment for H3K9me2, compared to input chromatin and

controls. H3K9me2 levels in chromatin derived from *Su(var)3-9*^{null} mutant tissues were significantly reduced (6- to 226-fold) compared to wild type. c) and d) ChIP analysis of two modifications associated with 'active' or 'open' chromatin (H3K9ac and H3K4me2). Small enrichment for these modifications was observed on repeated DNAs in wild type chromatin, compared to input and single copy controls. For most of the repeated DNAs, levels were not significantly altered in *Su(var)3-9*^{null} mutant chromatin ($p>0.5$ for all regions). H3K9ac levels were significantly increased in 5S rDNA in the mutants ($p<0.05$), and H3K4me2 was significantly decreased for the 1.688 satellite ($p<0.05$). Values are averages of 2 experiments.

Figure 5 Levels of extrachromosomal repeated DNAs are significantly increased in *Su(var)3-9*^{null} mutant tissues compared to wild type. a) Extrachromosomal DNA was isolated from wild type and *Su(var)3-9*^{null} mutant larvae using the Hirt supernatant method, and PCR reactions, terminated at logarithmic phase of amplification, were performed to evaluate the amounts of ecc DNA corresponding to specific sequences (see Materials and Methods). The gel shows an example of the PCR reactions for the specific regions examined. Ecc DNAs from the single-copy genes (actin and HDAC3) were not detected in either wild type or mutant larvae. The asterisk indicates that the band in the 1.688 satellite lane corresponds to the primers, not the PCR products. b) Quantitation demonstrates that the amount of ecc DNA for the 1.688 satellite and different regions of the rDNA are significantly higher in *Su(var)3-9*^{null} mutants compared to wild type (20- to 78-fold enrichment); the increase for 5S rDNA was only 2-fold, because wild type larvae contain high levels of ecc 5S rDNA. The values were averages of 3 sample extractions. c) Quantitation of PCR products indicates that the amount of ecc DNA in *Su(var)3-9*^{null} mutant diploid cells is about two-fold higher than in wild type. The values were averages of 3 sample extractions, and p values were <0.05 for the regions examined.

Figure 6 The RNAi pathway is also required to maintain the structural integrity of repeated DNAs and the nucleolus. a) Combined rDNA FISH (red) and fibrillarin IF (green) shows that *dcr-2*^{L811fsx} polytene nuclei contain multiple rDNA foci and ectopic nucleoli. b) Graph shows the average number of nucleoli in different RNAi mutants examined. Mutations at all loci contained significantly more nucleoli than wild type ($p<0.001$, except *aub*^{QC42} $p<0.004$). The *hls*^{del215} allele of *SpnE* had a mild phenotype ($p = 0.083$) c) ChIP analysis reveals reduced H3K9me2 levels in *dcr-2*^{L811fsx} chromatin compared to wild type ($p<0.05$), more so for rDNA than the 5S rDNA and satellite 1.688. Values are averages of 4 PCR reactions from 2 ChIP experiments. d) IF for H3K9me2 (red) and fibrillarin (green) on whole-mount brains and imaginal discs from wild type and *dcr-2*^{L811fsx} mutants. H3K9me2 localizes predominantly in DAPI-bright heterochromatin regions in wild type, but is more broadly distributed in *dcr-2*^{L811fsx} nuclei. Scale bar is 5μm. e) Ecc rDNA levels in *dcr-2*^{L811fsx} mutant larvae are significantly higher than in wild type (13- to 29-fold increases), but ecc DNA levels for 5S rDNA and satellite 1.688 did not increase.

Figure 7 Ligase 4 mutations partially suppresses ectopic nucleolus formation in *Su(var)3-9* mutants. Average nucleolus number of *Lig4*^{null}*; Su(var)3*-9^{null} polytene nuclei is 1.7 (N=83), which is significantly lower ($p<0.001$) than the average 2.7 (N=54) nucleoli observed in *Su(var)3-9*^{null} mutant nuclei.

Figure 8 Levels of extrachromosomal DNAs do not increase in *smc1*^{exc46l} mutant tissues, even though SMC1 protein levels are reduced in *Su(var)3-9*^{null} chromatin. a) ChIP analysis shows SMC1 levels (relative to wild type) in *Su(var)3-9*^{null} chromatin; values were averages of 4 PCR reactions from 2 ChIP experiments. SMC1 levels in *Su(var)3-9*^{null} chromatin were significantly lower than in wild type ($p<0.05$ for all repeated DNA except 5S rDNA). b) The amount of ecc DNA from satellite 1.688 and rDNA in *smc1*^{exc46l} mutant tissues do not differ significantly from wild type.

Figure 9 A model for regulation of nuclear architecture by the H3K9 methylation and RNAi pathways. In wild type diploid and polytene nuclei, the majority of the heterochromatin contains H3K9me2, and a single nucleolus forms around the rDNA. Loss of H3K9me2 from repeated DNA, due to *Su(var)3-9*, *HP1* or RNAi mutations, causes chromatin decondensation and elevated homologous recombination between repeat DNA copies. The recombination process results in formation of extrachromosomal DNAs that localize throughout the nucleoplasm, causing dispersal of satellite DNAs (not shown) and, in the case of rDNA, the formation of ectopic nucleoli. Decondensation is proposed to be primarily responsible for the 'lobed' structure of rDNA and nucleoli in diploid cells, with a minor contribution from low levels of ecc rDNA formation (dotted line). In polytene cells, decondensation is likely to be a prerequisite for increased recombination, but the much higher levels of ecc rDNA is proposed to generate the majority of the ectopic nucleoli.

References

1. Francastel, C., Schubeler, D., Martin, D.I. & Groudine, M. Nuclear compartmentalization and gene activity. *Nat Rev Mol Cell Biol* **1**, 137-43 (2000).
2. Cremer, T. & Cremer, C. Chromosome territories, nuclear architecture and gene regulation in mammalian cells. *Nature Reviews Genetics* **2**, 292 (2001).
3. John, B. The biology of heterochromatin. in *Heterochromatin: Molecular and Structural Aspects* (ed. Verma, R.S.) 1-147 (Cambridge University Press, Cambridge, 1988).
4. Jenuwein, T. & Allis, C.D. Translating the histone code. *Science* **293**, 1074-80 (2001).
5. Martin, C. & Zhang, Y. The diverse functions of histone lysine methylation. *Nat Rev Mol Cell Biol* **6**, 838-49 (2005).
6. Muller, H.J. Types of visible variations induced by X-rays in Drosophila. *J. Genet.* **22**, 299-334 (1930).
7. Schotta, G., Ebert, A., Dorn, R. & Reuter, G. Position-effect variegation and the genetic dissection of chromatin regulation in Drosophila. *Semin Cell Dev Biol* **14**, 67-75 (2003).
8. Pal-Bhadra, M. et al. Heterochromatic silencing and HP1 localization in Drosophila are dependent on the RNAi machinery. *Science* **303**, 669-72 (2004).
9. Grewal, S.I. & Moazed, D. Heterochromatin and epigenetic control of gene expression. *Science* **301**, 798-802 (2003).
10. Karpen, G.H., Schaefer, J.E. & Laird, C.D. A Drosophila rRNA gene located in euchromatin is active in transcription and nucleolus formation. *Genes Dev* **2**, 1745-63 (1988).
11. Santoro, R., Li, J. & Grummt, I. The nucleolar remodeling complex NoRC mediates heterochromatin formation and silencing of ribosomal gene transcription. *Nat Genet* **32**, 393-6 (2002).
12. Pikaard, C.S. The epigenetics of nucleolar dominance. *Trends Genet* **16**, 495-500 (2000).
13. Hawley, R.S. & Marcus, C.H. Recombinational controls of rDNA redundancy in Drosophila. *Annu Rev Genet* **23**, 87-120 (1989).
14. Blander, G. & Guarente, L. The Sir2 family of protein deacetylases. *Annu Rev Biochem* **73**, 417-35 (2004).
15. Tollervey, D., Lehtonen, H., Jansen, R., Kern, H. & Hurt, E.C. Temperature-sensitive mutations demonstrate roles for yeast fibrillarin in pre-rRNA processing, pre-rRNA methylation, and ribosome assembly. *Cell* **72**, 443 (1993).
16. Spradling, A. & Orr-Weaver, T. Regulation of DNA replication during Drosophila development. *Annu Rev Genet* **21**, 373-403 (1987).
17. Schotta, G. et al. Central role of Drosophila SU(VAR)3-9 in histone H3-K9 methylation and heterochromatic gene silencing. *Embo J* **21**, 1121-31 (2002).
18. Hirt, B. Selective extraction of polyoma DNA from infected mouse cell cultures. *J Mol Biol* **26**, 365-9 (1967).
19. Pont, G., Degroote, F. & Picard, G. Some extrachromosomal circular DNAs from Drosophila embryos are homologous to tandemly repeated genes. *J Mol Biol* **195**, 447-51 (1987).
20. Aravin, A.A. et al. The Small RNA Profile during Drosophila melanogaster Development. *Developmental Cell* **5**, 337 (2003).
21. Lee, Y.S. et al. Distinct Roles for Drosophila Dicer-1 and Dicer-2 in the siRNA/miRNA Silencing Pathways. *Cell* **117**, 69 (2004).
22. Lin, Y.H. & Keil, R.L. Mutations affecting RNA polymerase I-stimulated exchange and rDNA recombination in yeast. *Genetics* **127**, 31-8 (1991).
23. Cohen, S., Yacobi, K. & Segal, D. Extrachromosomal circular DNA of tandemly repeated genomic sequences in Drosophila. *Genome Res* **13**, 1133-45 (2003).
24. Cohen, Z., Bacharach, E. & Lavi, S. Mouse major satellite DNA is prone to eccDNA formation via DNA Ligase IV-dependent pathway. *Oncogene* (2006).

25. Kobayashi, T. & Ganley, A.R. Recombination regulation by transcription-induced cohesin dissociation in rDNA repeats. *Science* **309**, 1581-4 (2005).
26. Nonaka, N. et al. Recruitment of cohesin to heterochromatic regions by Swi6/HP1 in fission yeast. *Nat Cell Biol* **4**, 89-93 (2002).
27. Losada, A., Hirano, M. & Hirano, T. Identification of Xenopus SMC protein complexes required for sister chromatid†cohesion. *Genes Dev. %R 10.1101/gad.12.13.1986* **12**, 1986-1997 (1998).
28. Vakoc, C.R., Mandat, S.A., Olenchock, B.A. & Blobel, G.A. Histone H3 lysine 9 methylation and HP1gamma are associated with transcription elongation through mammalian chromatin. *Mol Cell* **19**, 381-91 (2005).
29. Sullivan, B.A. & Karpen, G.H. Centromeric chromatin exhibits a histone modification pattern that is distinct from both euchromatin and heterochromatin. *Nat Struct Mol Biol* **11**, 1076-83 (2004).
30. Cam, H.P. et al. Comprehensive analysis of heterochromatin- and RNAi-mediated epigenetic control of the fission yeast genome. *Nat Genet* **37**, 809-19 (2005).
31. Shankaranarayana, G.D., Motamedi, M.R., Moazed, D. & Grewal, S.I. Sir2 regulates histone H3 lysine 9 methylation and heterochromatin assembly in fission yeast. *Curr Biol* **13**, 1240-6 (2003).
32. Jackson, P.K. A new RING for SUMO: wrestling transcriptional responses into nuclear bodies with PIAS family E3 SUMO ligases. *Genes Dev* **15**, 3053-8 (2001).
33. Hari, K.L., Cook, K.R. & Karpen, G.H. The Drosophila *Su(var)2-10* Locus Encodes A Member of the PIAS Protein Family and Regulates Chromosome Structure and Function. *Genes and Development* **15**, 1334-48 (2001).
34. Nacerddine, K. et al. The SUMO Pathway Is Essential for Nuclear Integrity and Chromosome Segregation in Mice. *Developmental Cell* **9**, 769 (2005).
35. Peters, A.H. et al. Loss of the Suv39h histone methyltransferases impairs mammalian heterochromatin and genome stability. *Cell* **107**, 323-37 (2001).
36. McKee, B.D. & Karpen, G.H. Drosophila ribosomal RNA genes function as an X-Y pairing site during male meiosis. *Cell* **61**, 61-72 (1990).
37. Karpen, G.H., Le, M.H. & Le, H. Centric heterochromatin and the efficiency of achiasmate disjunction in Drosophila female meiosis. *Science* **273**, 118-22 (1996).
38. Dernburg, A.F., Sedat, J.W. & Hawley, R.S. Direct evidence of a role for heterochromatin in meiotic chromosome segregation. *Cell* **86**, 135-46 (1996).
39. Cartwright, I.L. et al. Analysis of Drosophila chromatin structure in vivo. *Methods Enzymol* **304**, 462-96 (1999).
40. Critchlow, S.E., Bowater, R.P. & Jackson, S.P. Mammalian DNA double-strand break repair protein XRCC4 interacts with DNA ligase IV. *Curr Biol* **7**, 588-98 (1997).
41. Glaser, R.L., Karpen, G.H. & Spradling, A.C. Replication forks are not found in a Drosophila minichromosome demonstrating a gradient of polytenization. *Chromosoma* **102**, 15-9 (1992).
42. Ivessa, A.S., Zhou, J.Q. & Zakian, V.A. The Saccharomyces Pif1p DNA helicase and the highly related Rrm3p have opposite effects on replication fork progression in ribosomal DNA. *Cell* **100**, 479-89 (2000).
43. Westphal, T. & Reuter, G. Recombinogenic effects of suppressors of position-effect variegation in Drosophila. *Genetics* **160**, 609-21 (2002).
44. Kaeberlein, M., McVey, M. & Guarente, L. The SIR2/3/4 complex and SIR2 alone promote longevity in Saccharomyces cerevisiae by two different mechanisms. *Genes Dev* **13**, 2570-80 (1999).
45. Osipovich, O. et al. Targeted inhibition of V(D)J recombination by a histone methyltransferase. *Nat Immunol* **5**, 309-16 (2004).
46. Peters, A.H.F.M. et al. Partitioning and Plasticity of Repressive Histone Methylation States in Mammalian Chromatin. *Molecular Cell* **12**, 1577 (2003).

47. Dorsett, D. et al. Effects of sister chromatid cohesion proteins on cut gene expression during wing development in Drosophila. *Development* **132**, 4743-4753 (2005).
48. Austin, R.J., Orr-Weaver, T.L. & Bell, S.P. Drosophila ORC specifically binds to ACE3, an origin of DNA replication control element. *Genes Dev* **13**, 2639-49 (1999).
49. Kuschak, T.I., Kuschak, B.C., Smith, G.M., Wright, J.A. & Mai, S. Isolation of extrachromosomal elements by histone immunoprecipitation. *Biotechniques* **30**, 1064-8, 1070-2 (2001).

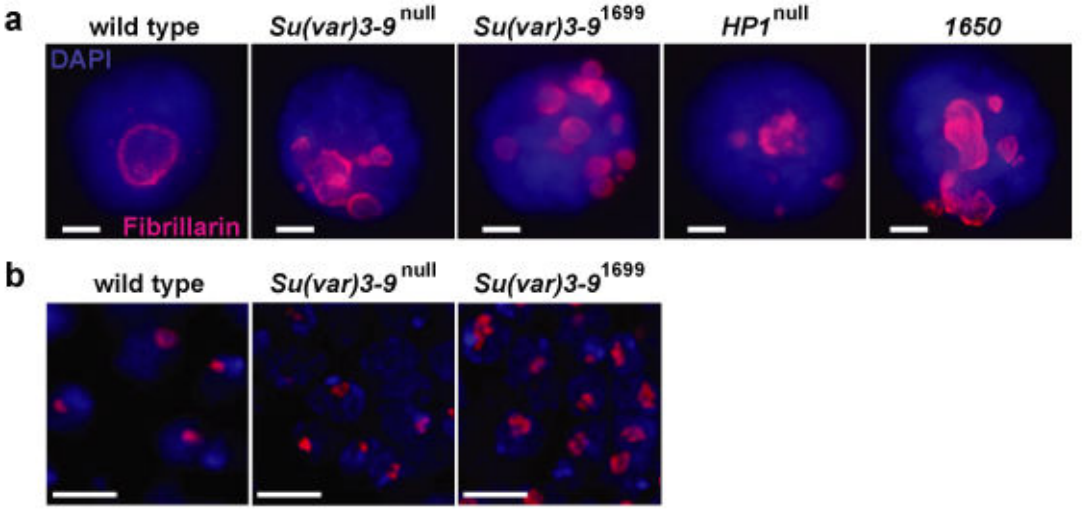

Figure 1 *Su(var)* mutants contain multiple nucleoli. a) IF with antibodies against the nucleolus marker fibrillarin (red) in whole-mount nuclei of salivary glands from wild-type, *Su(var)3-9*^{null}, *Su(var)3-9*^{1699}, *HP1*^{null} and *Su(TDA-PEV)1650* homozygous mutants. Wild type cells have one nucleolus, whereas the mutants display multiple nucleoli. Blue = DAPI. Scale bars are 10μm. b) Fibrillarin IF in whole-mount imaginal disc and brain tissues from wild type and *Su(var)3-9* mutants are shown. The single, wild type nucleolus (N=51) tended to be round, whereas nucleoli in the mutants are irregular (lobed) and larger. Quantitative analysis showed that 44% of *Su(var)3-9*^{null} mutant nuclei contained lobed nucleoli (N=55), versus 10% for wild-type ($p<0.001$). The scale bars are 5μm.

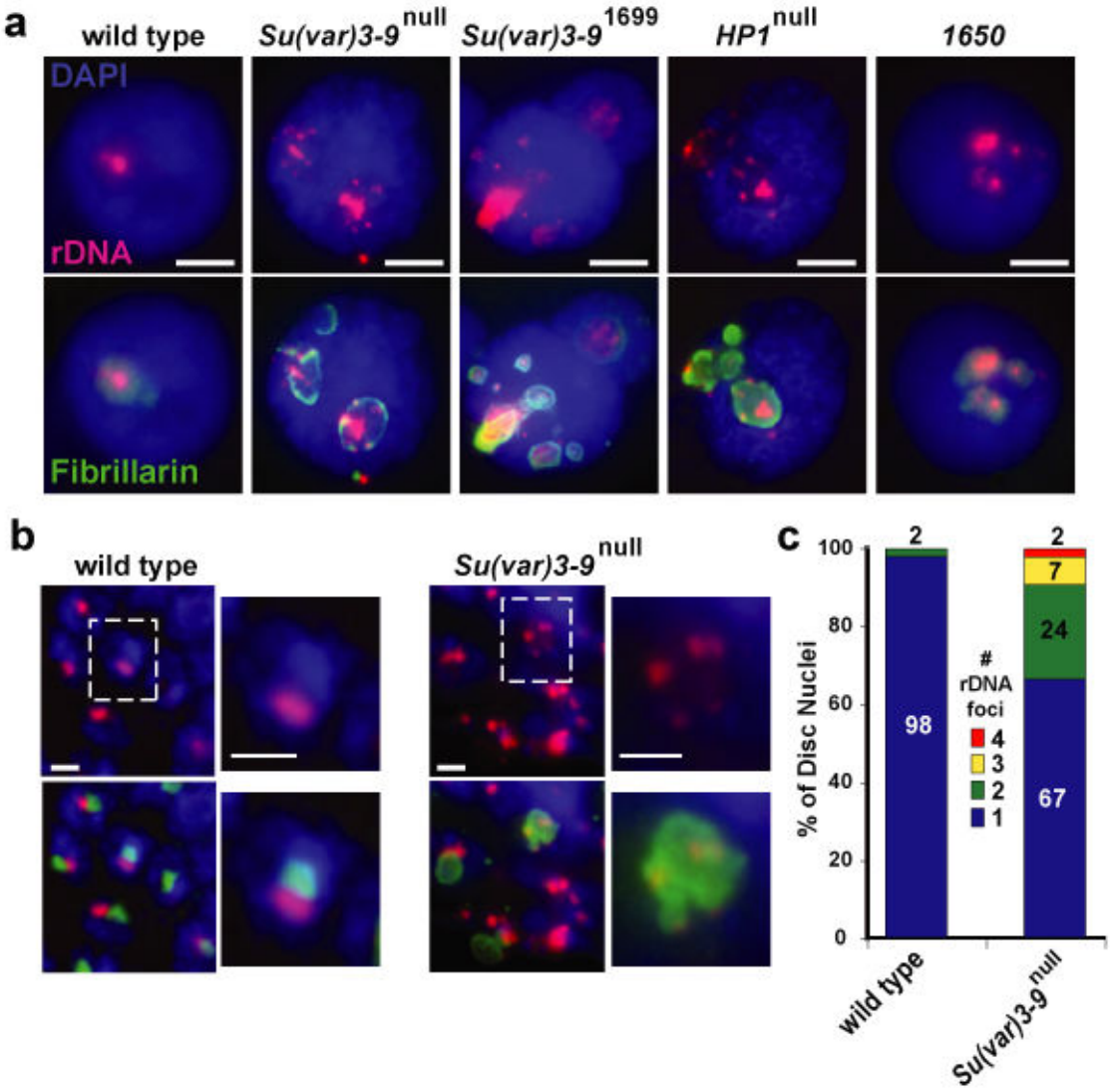

Figure 2 *Su(var)* mutants have dispersed rDNA foci, each of which forms an ectopic nucleolus.
a) Fluorescence in situ hybridization (FISH) for rDNA (red) and IF for fibrillarin (green) were performed on whole-mount salivary glands from wild type, *Su(var)3-9*^{null}, *Su(var)3-9*^{1699}, *HP1*^{null}, and *Su(TDA-PEV)1650* homozygous mutants. Blue = DAPI. There is a single site of rDNA in >98% of wild type nuclei, whereas the *Su(var)* mutant nuclei contain multiple rDNA foci, which are all surrounded by fibrillarin. Scale bars are 15μm.
b) Combined rDNA FISH (red) and fibrillarin IF (green) analysis of whole-mount imaginal disc and brain tissues from wild type and *Su(var)3-9*^{null} mutant larvae. Wild type nucleoli contain a single, compact rDNA focus, whereas *Su(var)3-9*^{null} mutants frequently display multiple rDNA foci. Scale bars are 3μm.
c) Quantitative analysis of the number of rDNA foci in wild type and *Su(var)3-9*^{null} diploid nuclei. 98% of wild type cells (N=96) contain one rDNA signal, compared to 67% of *Su(var)3-9*^{null} nuclei, and the percent with 2, 3, and 4 rDNA signals was 24%, 7%, and 2%, respectively (average =1.44 ± 0.73 rDNA foci per mutant nucleus, N=53, $p<0.001$)

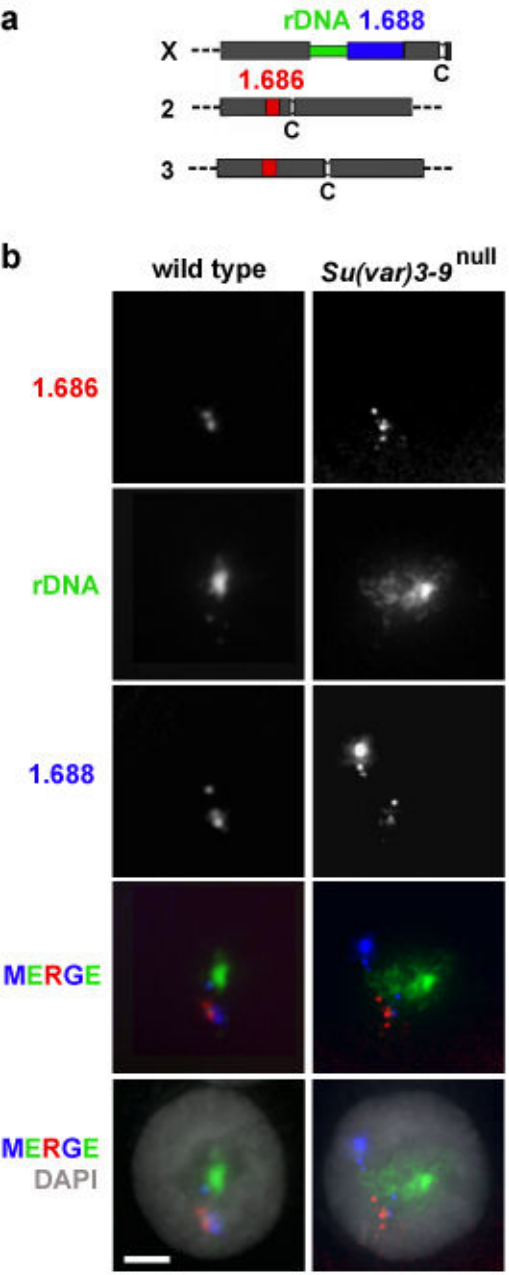

Figure 3 Satellite DNA organization is disrupted in *Su(var)3-9*^{null} mutant nuclei. a) Locations of rDNA and satellite DNAs in the *Drosophila melanogaster* genome (not to scale). The rDNA is located in the heterochromatin of the X and Y sex chromosomes, the 1.688 satellite (359-bp repeats) are next to the X rDNA, and the 1.686 satellite is in the heterochromatin of chromosomes 2 and 3. b) FISH was performed on whole-mount polytene salivary glands isolated from wild type and *Su(var)3-9*^{null} mutants. In wild type nuclei, specific satellite DNAs are organized in single sites, and the different satellite signals are close to each other. In *Su(var)3-9*^{null} mutant nuclei, individual satellite DNAs are dispersed to multiple sites and are not clustered with other satellites. Gray is DAPI, FISH probe colors correspond to the diagram in a. Scale bars are 15μm. c) The number of 1.688 and 1.686 foci were significantly higher in mutant nuclei compared to wild type ($p<0.001$). d) Distances between satellite signals were quantitated in 3-dimensional reconstructions. The intra-satellite distances in *Su(var)3-9*^{null} mutant nuclei were significantly higher than in wild type ($p<0.001$).

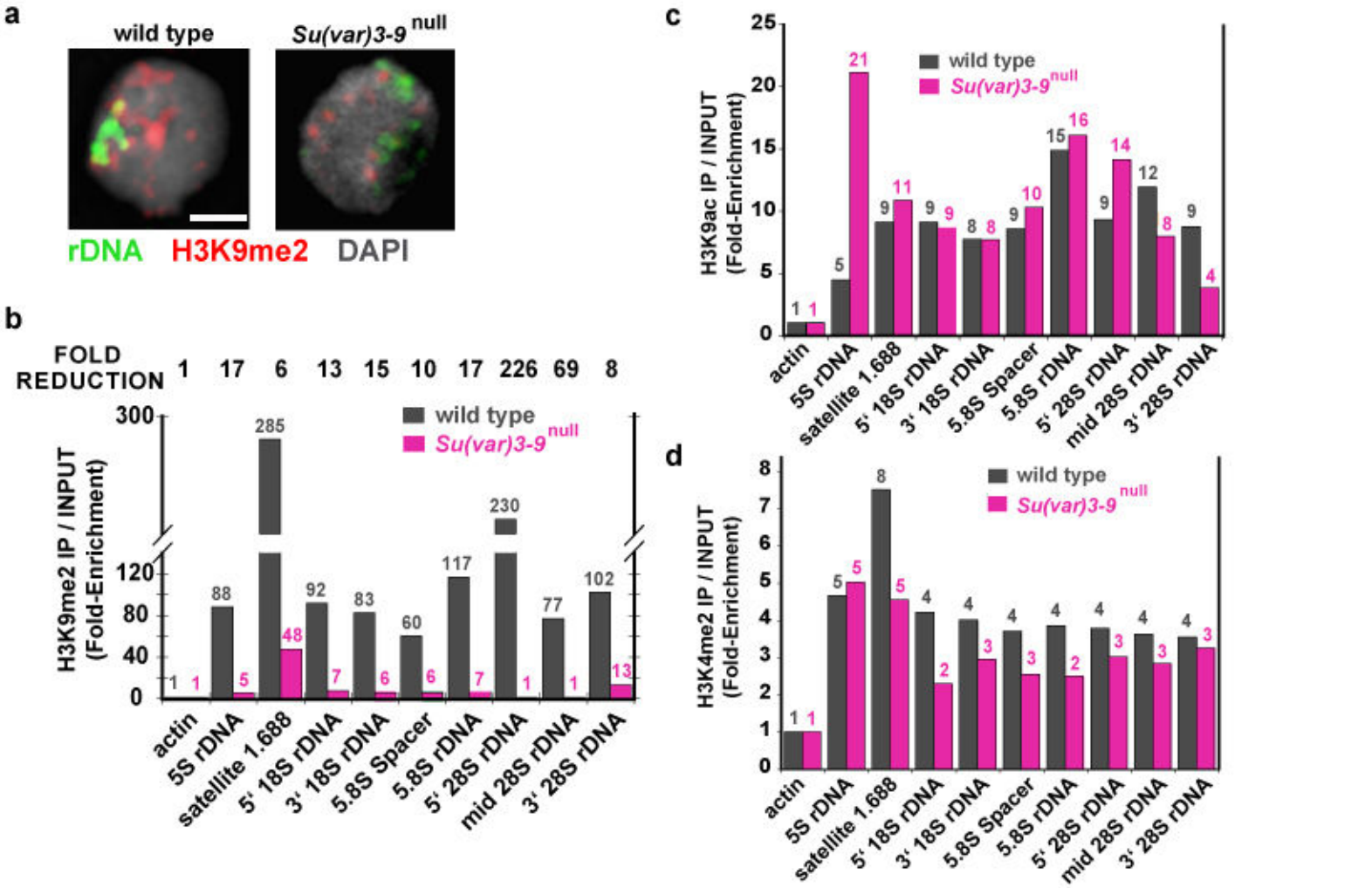

Figure 4 Analysis of histone modifications in chromatin containing repeated DNA in wild type and *Su(var)3-9*^{null} cells. a) IF using antibodies that specifically bind H3K9me2 (red) combined with FISH for rDNA (green) in squashed diploid nuclei. In wild type nuclei, rDNA chromatin partially overlaps with the H3K9me2 signals (correlation coefficient = 0.61± 0.08), and the amount of overlap was significantly reduced in *Su(var)3-9*^{null} mutants (correlation coefficient = 0.40 ± 0.03; $p<0.01$). Scale bar is 3µm. b) Chromatin immunoprecipitation (ChIP) analysis of H3K9me2 levels in wild type and *Su(var)3-9*^{null} mutant imaginal disc tissues. The graph shows H3K9me2 levels for the repeated DNAs examined by PCR, standardized to actin and HDAC single copy controls (see Materials and Methods); values were averages of 5 ChIP experiments. In wild type cells, the 1.688 satellite (359-bp repeats), 5S rDNA (in chromosome 2 euchromatin), and the rDNA on the sex chromosomes contain significant enrichment for H3K9me2, compared to input chromatin and controls. H3K9me2 levels in chromatin derived from *Su(var)3-9*^{null} mutant tissues were significantly reduced (6- to 226-fold) compared to wild type. c) and d) ChIP analysis of two modifications associated with 'active' or 'open' chromatin (H3K9ac and H3K4me2). Small enrichment for these modifications was observed on repeated DNAs in wild type chromatin, compared to input and single copy controls. For most of the repeated DNAs, levels were not significantly altered in *Su(var)3-9*^{null} mutant chromatin ($p>0.5$ for all regions). H3K9ac levels were significantly increased in 5S rDNA in the mutants ($p<0.05$), and H3K4me2 was significantly decreased for the 1.688 satellite ($p<0.05$). Values are averages of 2 experiments.

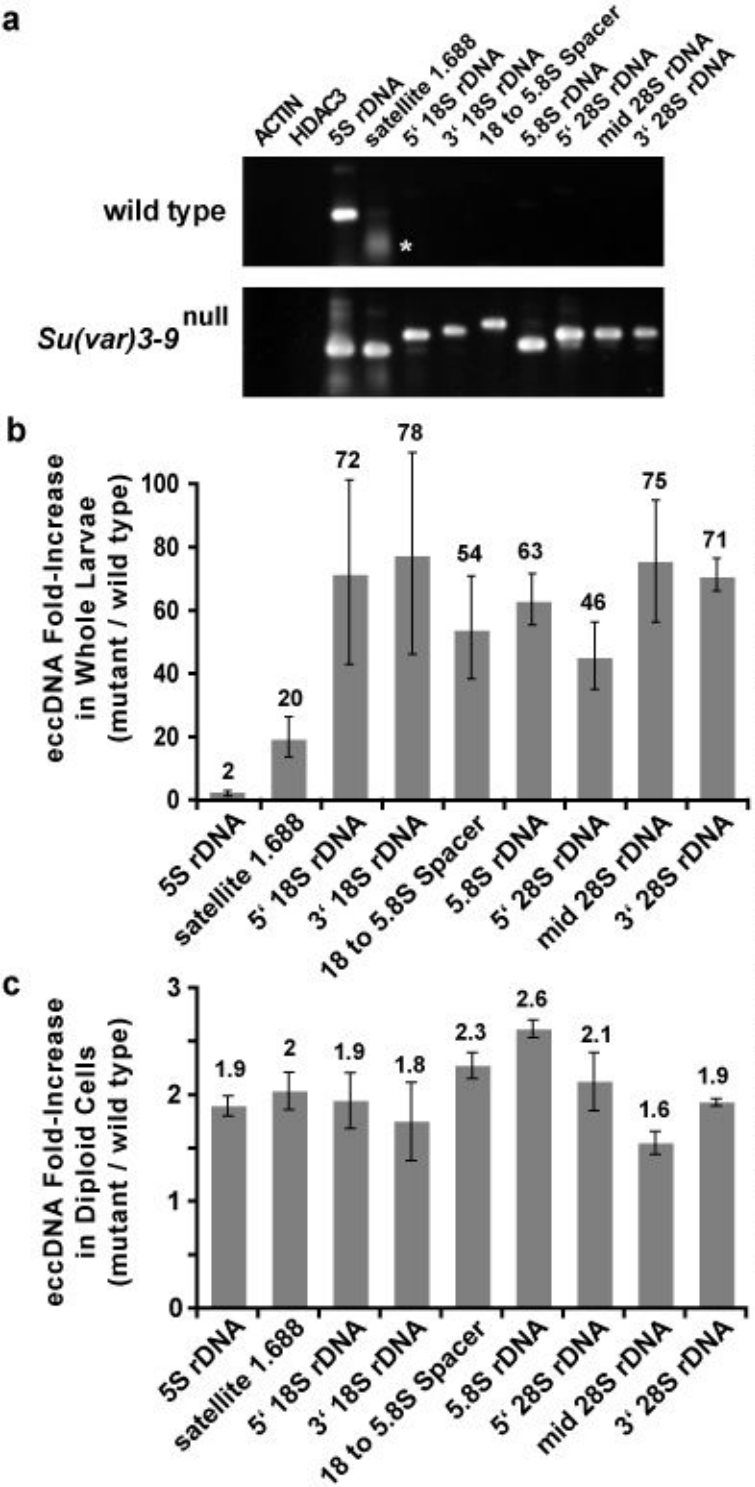

Figure 5 Levels of extrachromosomal repeated DNAs are significantly increased in *Su(var)3-9*^{null} mutant tissues compared to wild type. a) Extrachromosomal DNA was isolated from wild type and *Su(var)3-9*^{null} mutant larvae using the Hirt supernatant method, and PCR reactions, terminated at the logarithmic phase of amplification, were performed to evaluate the amounts of ecc DNA corresponding to specific sequences (see Materials and Methods). The gel shows an example of the PCR reactions for the specific regions examined. Ecc DNAs from the single-copy genes (actin and HDAC3) were not detected in either wild-type or mutant larvae. The asterisk indicates that the band in the 1.688 satellite lane corresponds to the primers, not the PCR products. b) Quantitation demonstrates that the amount of ecc DNA for the 1.688 satellite and different regions of the rDNA are significantly higher in *Su(var)3-9*^{null} mutants compared to wild type (20- to 78-fold enrichment); the increase for 5SrDNA was only 2-fold, because wild type larvae contain high levels of ecc 5S rDNA. The values were averages of 3 sample extractions. c) Quantitation of PCR products indicates that the amount of ecc DNA in *Su(var)3-9*^{null} mutant diploid cells is about 2-fold higher than in wild type. The values were averages of 3 sample extractions, and p values were <0.05 for the regions examined.

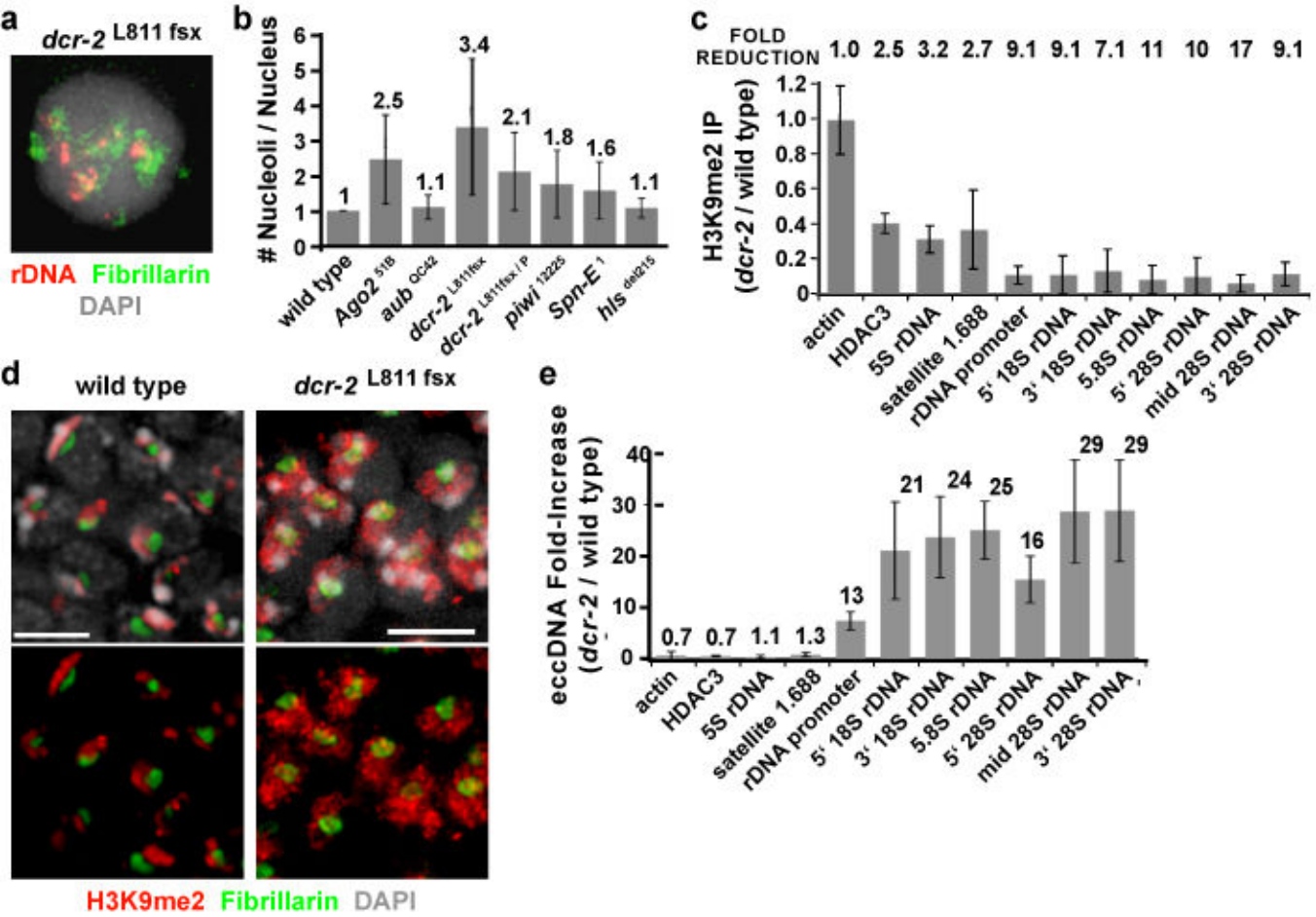

Figure 6 The RNAi pathway is also required to maintain the structural integrity of repeated DNAs and the nucleolus. a) Combined rDNA FISH (red) and fibrillarin IF (green) shows that *dcr-2*^{L811fsx} polytene nuclei contain multiple rDNA foci and ectopic nucleoli. b) Graph shows the average number of nucleoli in different RNAi mutants examined. Mutations at all loci contained significantly more nucleoli than wild type ($p<0.001$, except *aub*^{QC42} $p<0.004$). The *hls*^{del215} allele of *SpnE* had a mild phenotype ($p = 0.083$). c) IF for H3K9me2 (red) and fibrillarin (green) on whole-mount brains and imaginal discs from wild type and *dcr-2*^{L811fsx} mutants. H3K9me2 localizes predominantly in DAPI-bright heterochromatin regions in wild type, but is more broadly distributed in *dcr-2*^{L811fsx} nuclei. Scale bar is 5µm. d) ChIP analysis reveals reduced H3K9me2 levels in *dcr-2*^{L811fsx} chromatin compared to wild type ($p<0.05$), more so for rDNA than the 5S rDNA and satellite 1.688. Values are averages of 4 PCR reactions from 2 ChIP experiments. e) Ecc rDNA levels in *dcr-2*^{L811fsx} mutant larvae are significantly higher than in wild type (13- to 29-fold increases), but ecc DNA levels for 5S rDNA and satellite 1.688 did not increase.

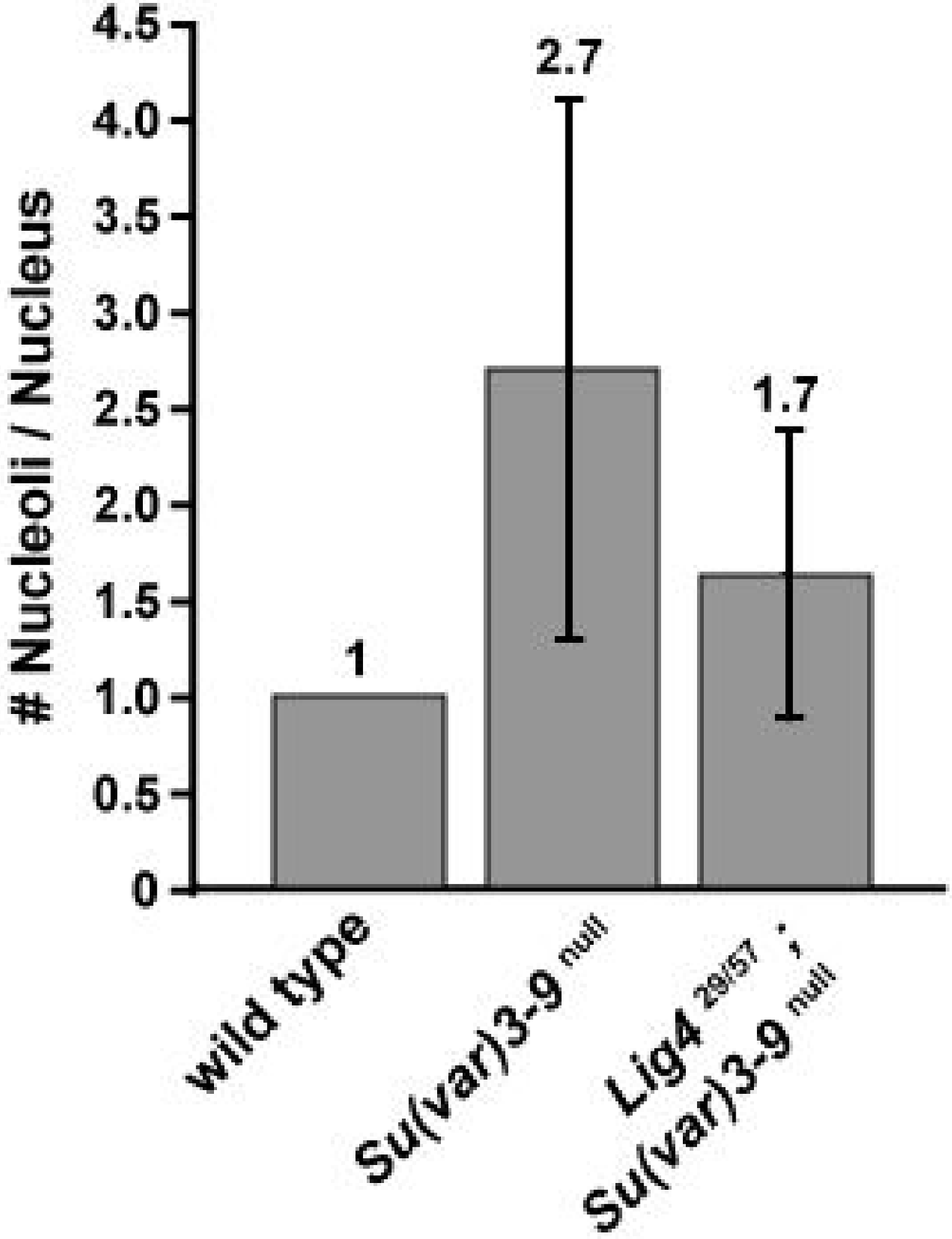

Figure 7 Ligase 4 mutations partially suppress ectopic nucleolus formation in *Su(var)3-9* mutants. Average nucleolus number of *Lig4*^{null}; *Su(var)3-9*^{null} polytene nuclei is 1.7 (N=83), which is significantly lower ($p<0.001$) than the average 2.7 nucleoli (N=54) observed in *Su(var)3-9*^{null} mutant nuclei.

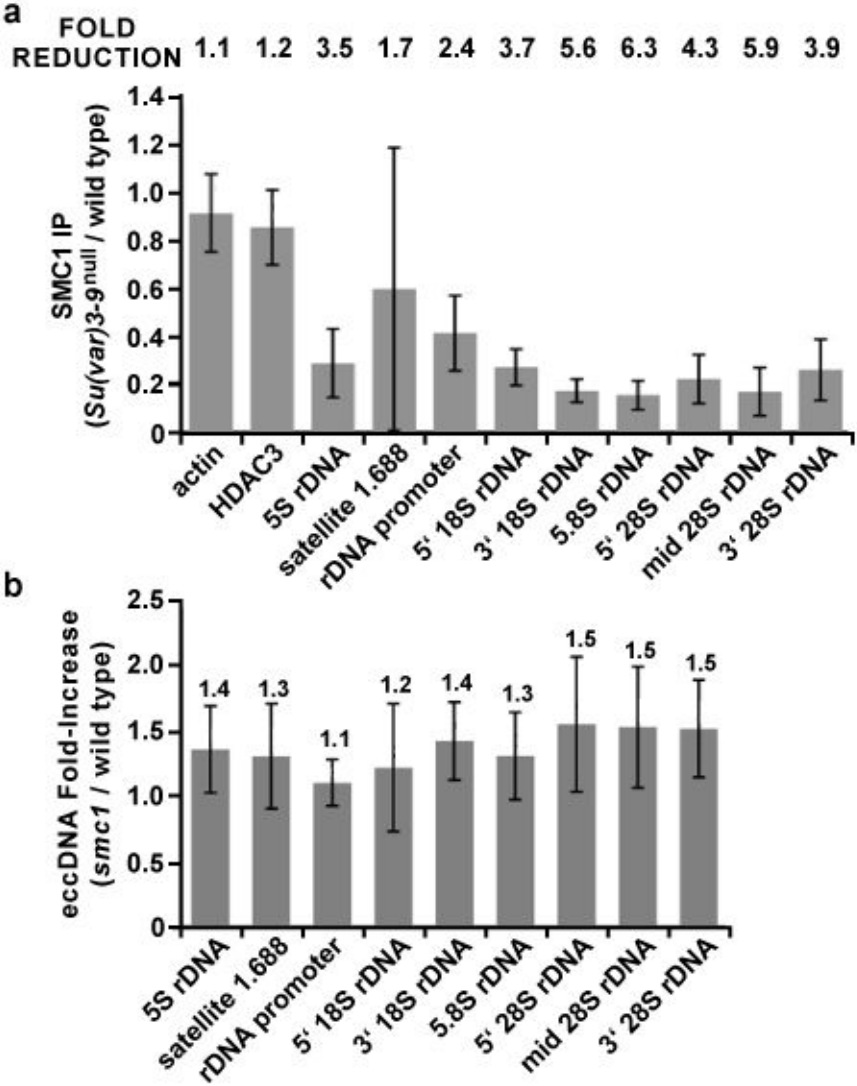

Figure 8 Levels of extrachromosomal DNAs do not increase in *smc1*^{exc45} mutant tissues, even though SMC1 protein levels are reduced in *Su(var)3-9*^{null} chromatin. a) ChIP analysis shows SMC1 levels (relative to wild type) in *Su(var)3-9*^{null} chromatin; fold-reduction is shown above. Values were averages of 4 PCR reactions from 2 ChIP experiments. SMC1 levels in *Su(var)3-9*^{null} chromatin were significantly lower than in wild type ($p<0.05$ for all repeated DNA except 5S rDNA). b) The amount of ecc DNA from satellite 1.688 and rDNA in *smc1*^{exc45} mutant tissues do not significantly differ from wild type.

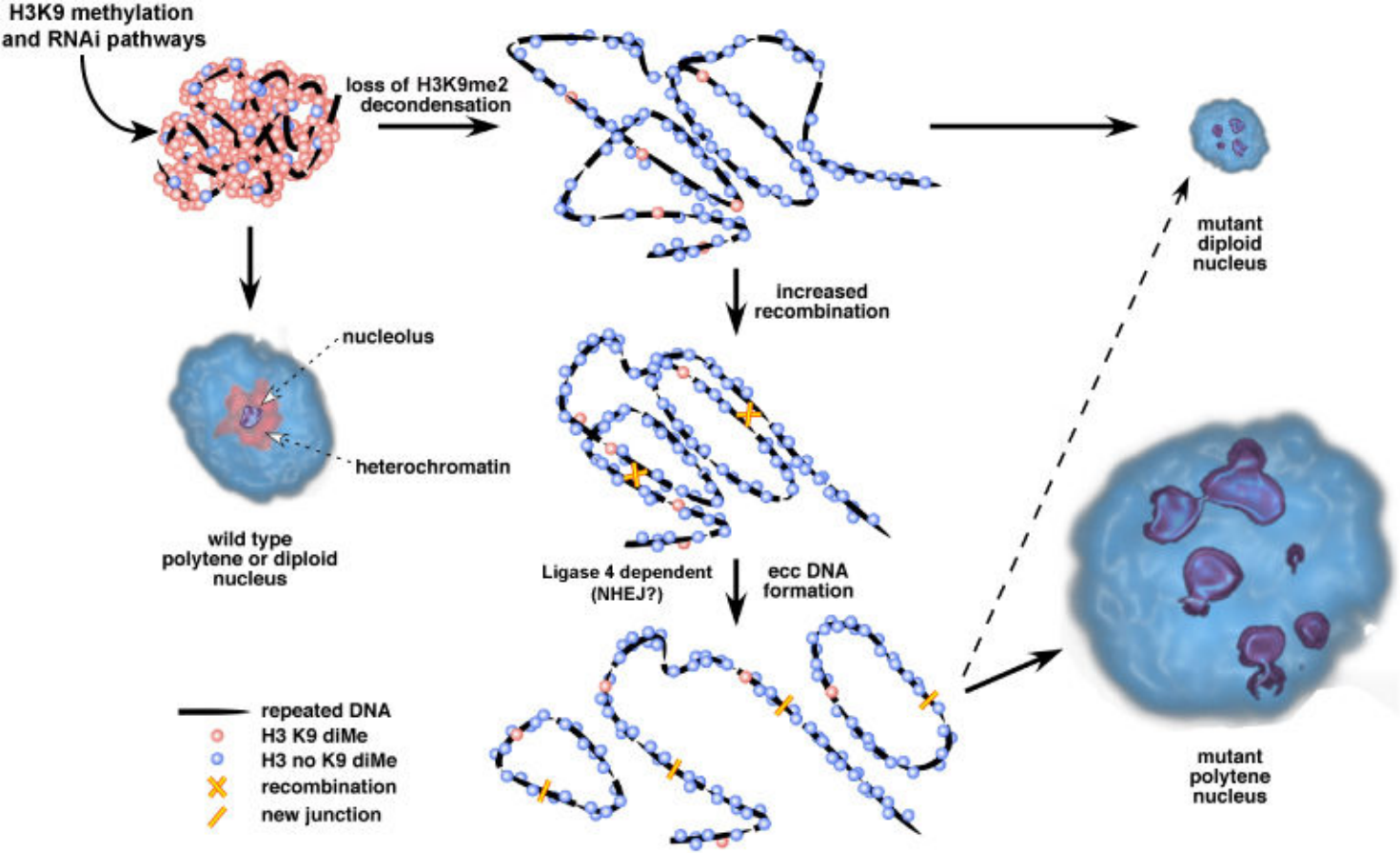

Figure 9 A model for regulation of nuclear architecture by the H3K9 methylation and RNAi pathways. In wild type diploid and polytene nuclei, the majority of the heterochromatin contains H3K9me2, and a single nucleolus forms around the rDNA. Loss of H3K9me2 from repeated DNA, due to *Su(var)3-9, HP1* or RNAi mutations, causes chromatin decondensation and elevated homologous recombination between repeat DNA copies. Recombination results in formation of extrachromosomal DNA that localize throughout the nucleoplasm, causing dispersal of satellite DNAs (not shown) and, in the case of rDNA, the formation of ectopic nucleoli. Decondensation is proposed to be primarily responsible for the 'lobed' structure of rDNA and nucleoli in diploid cells, with a minor contribution from low levels of ecc rDNA formation (dotted line). In polytene cells, decondensation is likely to be a prerequisite for increased recombination, but the much higher levels of ecc rDNA is proposed to generate the majority of the ectopic nucleoli.